Published in final edited form as:
J Nucl Med. 2020 November 01; 61(11): 1678–1683. doi:10.2967/jnumed.120.242248.

Data-Driven Respiratory Gating Outperforms Device-Based Gating for Clinical FDG PET/CT

Matthew D Walker[1], **Andrew J Morgan**[1], **Kevin M Bradley**[2,3], **Daniel R McGowan**[1,4]

[1]Radiation Physics and Protection, Churchill Hospital, Oxford, UK

[2]Department of Radiology, Churchill Hospital, Oxford, UK

[3]Wales Research & Diagnostic PET Imaging Centre, Cardiff University, Cardiff, UK

[4]Department of Oncology, University of Oxford, Oxford, UK

Abstract

A data-driven method for respiratory gating in PET has recently been commercially developed. We sought to compare the performance of the algorithm to an external, device-based system for oncological ^{18}F-FDG PET/CT imaging.

Methods—144 whole-body ^{18}F-FDG PET/CT examinations were acquired using a Discovery D690 or D710 PET/CT scanner (GE Healthcare), with a respiratory gating waveform recorded by an external, device-based respiratory gating system. In each examination, two of the bed positions covering the liver and lung bases were acquired with duration of 6 minutes. Quiescent period gating retaining ~50% of coincidences was then able to produce images with an effective duration of 3 minutes for these two bed positions, matching the other bed positions. For each exam, 4 reconstructions were performed and compared: data-driven gating (*DDG-retro*), external device-based gating (*RPM-gated*), no gating but using only the first 3 minutes of data (*Ungated matched*), and no gating retaining all coincidences (*Ungated full*). Lesions in the images were quantified and image quality was scored by a radiologist, blinded to the method of data processing.

Results—The use of *DDG-retro* was found to increase SUV_{max} and to decrease the threshold-defined lesion volume in comparison to each of the other reconstruction options. Compared to RPM-gated, DDG-retro gave an average increase in SUV_{max} of 0.66±0.1 g/mL (n=87,p<0.0005). Although results from the blinded image evaluation were most commonly equivalent, *DDG-retro* was preferred over *RPM-gated* in 13% of exams while the opposite occurred in just 2% of exams. This was a significant preference for *DDG-retro* (p=0.008,n=121). Liver lesions were identified in 23 exams. Considering this subset of data, *DDG-retro* was ranked superior to *Ungated full* in 6/23 (26%) of cases. Gated reconstruction using the external device failed in 16% of exams, while *DDG-retro* always provided a clinically acceptable image.

First and Corresponding Author: Dr Matthew D Walker, Radiation Physics and Protection, Churchill Hospital, Oxford, OX3 7LE, UK. Telephone: + 44(0)1865 226718. matthew.walker@ouh.nhs.uk.

Disclaimer: This paper presents independent research funded by the NIHR and HEE. The views expressed are those of the authors and not necessarily those of the NHS, the NIHR, HEE or the Department of Health.

Disclosure
Oxford University Hospitals NHS Foundation Trust has a research contract with GE Healthcare covering loan of equipment, but without financial support. No other potential conflicts of interest relevant to this article exist.

Conclusion—In this clinical evaluation, the data-driven respiratory gating technique provided superior performance as compared to the external device-based system. For the majority of exams the performance was equivalent, but data-driven respiratory gating had superior performance in 13% of exams, leading to a significant preference overall.

Keywords

Respiratory gating; PET/CT; RPM; Data-Driven gating; FDG

Introduction

Respiratory motion leads to a degradation of image quality in clinical PET-CT. The amplitudes of the organ motions and deformations associated with respiration varies substantially between patients, with liver motions of 2–3 cm not uncommon(1,2). These amplitudes exceed the spatial resolutions of modern PET scanners(3). The respiratory period is typically in the range 3–6 seconds, which is far shorter than PET acquisition durations of 2–3 minutes per bed position. In the absence of respiratory gating, PET images are hence blurred by the motions of many respiratory cycles. This is particularly notable when imaging the upper abdomen and lower thorax. Despite this, respiratory gating has yet to be adopted as a standard requirement for routine clinical ^{18}F-FDG PET/CT imaging(3).

There are several approaches to respiratory gating in PET(4). Commercially available external devices can be used to track the motion of the chest wall and thus provide a respiratory waveform that can be used for gating. Such devices have been in clinical use for several years and include the camera-based, Real-time Position Management™ (RPM) Respiratory Gating system (Varian Medical Systems) and the pressure-belt based respiratory gating system AZ-733VI (Anzai Medical). An alternative approach is to extract a respiratory waveform from the PET data itself. Such a data-driven approach has recently been developed and commercialised by a scanner manufacturer (GE Healthcare), offering improved workflow with reduced patient setup time. The algorithm makes use of principal component analysis to extract a respiratory waveform from the PET data. Early versions of this method were developed and evaluated by Thielemans et al.(5–7). The commercial version has been evaluated in phantom studies where it was found to reliably provide a respiratory waveform(8). The quality of the waveforms extracted by the algorithm have been assessed from clinical ^{18}F-FDG PET data which shows an example of suitable and unsuitable waveforms(9). Clinical examples have also been published(8,10).

In the current study we performed a clinical evaluation of principal component analysis-based data-driven respiratory gating for ^{18}F-FDG PET-CT, with comparison to respiratory gating using an external device, and also to ungated data. Based on the fact that data-driven gating extracts a respiratory waveform from the 3-dimensional motion of the radioactivity within the internal organs (as opposed to tracking the rise and fall of the chest wall(11)), we hypothesised that the data-driven gating would provide images with improved mitigation of respiratory motion as compared to device-based gating using an external, camera-based tracking system(12,13). To our knowledge, this is the first large-scale evaluation of a data-driven gating algorithm that has been implemented for clinical use. Büther et al. (14)

Europe PMC Funders Author Manuscripts

recently evaluated a DDG algorithm developed for use with continuous bed motion acquisition, and demonstrated similar performance between DDG and device-based gating. Other DDG algorithms have been evaluated clinically but await commercial implementation (15,16).

Materials and Methods

Patient Selection

The study made use of 144 whole-body ^{18}F-FDG PET/CT examinations acquired in August 2018 at the Churchill Hospital, Oxford. They represent an unbiased sample of ^{18}F-FDG PET/CT examinations as performed at the Hospital, which is a regional, public cancer centre. The study was performed retrospectively and was approved by the Institutional Review Board and Health Research Authority (reference: 19/HRA/0315); the need for written informed consent was waived.

PET-CT Acquisition Protocol

Data were acquired using a Discovery 690 or Discovery 710 PET-CT scanner (GE Healthcare)(17). Following a minimum of 6-hours of fasting, patients received i.v. administration of 4 MBq/kg body weight ^{18}F-FDG. They rested for a 90 minute uptake period before commencement of the PET-CT acquisition. A marker block was attached to the patient's chest, allowing for respiratory motion to be tracked by an infra-red camera (RPM) that was attached at the foot-end of the patient couch. A scout scan was acquired, from which two bed positions were identified by the PET/CT technologist for application of respiratory gating. These bed positions were the two positions that covered the liver and the base of the lungs. A free-breathing, helical CT was then acquired followed by the PET.

The acquisition duration for the two bed positions with respiratory gating was set to 6-min per bed. This was chosen such that on application of quiescent period respiratory gating, with retention of ~50% of coincidences, an effective acquisition duration of 3 minutes per bed position was maintained. The other bed positions, where respiratory gating was not intended, had acquisition durations set to 3 minutes. The PET bed overlap was 23%.

Respiratory Gating and Image Reconstruction

The manufacturer's Bayesian penalized likelihood (BPL) reconstruction algorithm (Q.Clear) was used, with a β-value of 400(18), to create 4 PET data sets from each examination. These were reconstructed with: no respiratory gating retaining all data (termed *Ungated full*); no respiratory gating but retaining only the first 3 minutes from each of the two 6-minute bed positions (termed *Ungated matched*); quiescent period respiratory gated images (19) where gating is applied only to the two 6-minute bed positions, with the gating signal provided by the external device (termed *RPM-gated*); and similarly gated images but with the gating signal extracted from the PET data using the manufacturer's algorithm (MotionFree) (termed *DDG-retro*). For the *RPM-gated* and *DDG-retro* reconstructions, the manufacturer's quiescent period respiratory gating algorithm was used (Q.Static) with retention of ~50% of the data. As shown in Figure 1, this method retains data from the almost stationary period around the end of expiration, while discarding data from the inspiration phase associated

with most movement (19). For the *DDG-retro* reconstruction, the algorithm makes an assessment of the signal-to-noise of respiratory frequencies within the waveform. This quality metric is defined as the R value of the waveform(9). The waveforms were also inspected and scored by a medical physicist similar to our previous work(9). No threshold based on the R value (or visual score) was applied, with DDG applied to all datasets. The *Ungated full* reconstruction was included to investigate the trade-off between applying a respiratory motion correction which discards coincidences, compared to no motion correction but with a similarly extended acquisition time.

Clinical Evaluation

Lesions present in the region where respiratory gating was applied were identified by an experienced radiologist, blinded to the method of reconstruction, and used for assessment of SUV_{max}, SUVmean, and lesion volume as determined using a threshold set at 40% of SUV_{max}(16). For lesions where the contrast with the surrounding tissue was insufficient for this determination of lesion volume, only SUV_{max} was measured. This quantitative analysis was supplemented by a clinical evaluation performed by the radiologist, including a blinded side-by-side comparison of the four images from each exam. Images were displayed in a random order and then scored (scale of 1–6) and ranked in terms of the overall diagnostic image quality. Image quality scores were described as follows: 1=excellent, no/minimal heterogeneities; 2=very good, subtle, tiny heterogeneities; 3=good, small heterogeneities visible throughout; 4=satisfactory, some significant heterogeneities of varying size and magnitude; 5=numerous significant heterogeneities; 6=Non diagnostic. The noise in liver and bone marrow was also scored visually (scale of 1–6).

Statistical Analyses

To test for differences in the radiologist's clinical evaluation of image quality (ranks and scores) between the four groups, a Friedman test was performed. To test for differences in lesion uptake values and volume between the four groups, a one-way ANOVA with repeated measures was used. Due to the non-normal distribution of the lesion uptake values and volumes, these data were first transformed using the natural logarithm after which they were approximately normal prior to application of the ANOVA. When significant differences between groups were indicated by the Friedman test, or by the ANOVA including a Greenhouse-Geisser correction for violation of sphericity as per Mauchly's test, these differences were assessed using a Wilcoxon Signed Ranks Test (for the ordinal data) or a paired t-test (for the lesion uptake measures). For these post-hoc tests, a Bonferroni correction was applied with consideration of three planned tests (*DDG-retro* compared to the other three data sets), resulting in a critical p value of 0.017. The presented p-values are hence uncorrected for multiple comparisons but only considered significant if below 0.017. Statistical analyses were performed using SPSSv25.

Results

Device and Algorithm Performance

For examinations where the external gating system failed to provide a gating signal, *RPM-gated* images were either unable to be reconstructed or had substantial, obvious artefacts and

were discarded. The external device failed to record a usable respiratory trace in 23 of the 144 PET/CT examinations (16%). From the 288 bed positions (144 exams) to which DDG was applied, the derived waveforms had a mean R value of 17.4 and a median value of 16.0. 155 of the 288 waveforms (54%) had R values greater than 15, which is the manufacturer's recommended threshold above which DDG be applied. The DDG-derived waveforms were scored visually to be unsuitable for respiratory gating for 15 bed positions (from 13 exams). The waveforms were however generated and their use did not create image artefacts in the *DDG-retro* images. The external system failed in 3 of these 13 exams. Of the 15 DDG-derived waveforms considered unsuitable for gating, 4 had R values that were greater than 15, and 11 had R values that were less than 15. Eight of these 11 R-values were particularly low (R<6). According to this visual inspection, *DDG-retro* did not provide a robust respiratory trace for 15/288 = 5% of bed positions, as compared to RPM which failed for 16% of exams.

Lesion quantification

The use of *DDG-retro* was found to increase SUV_{max} and SUVmean and to decrease the threshold-defined lesion volume for this dataset while making comparison to each of the other reconstruction options. Paired differences in SUV_{max} are presented in Figure 2. The quantified uptake (SUV_{max}, SUVmean) and lesion volumes were all found to have significant differences between groups in the one-way, Greenhouse-Geisser corrected ANOVA as applied to the logarithmically transformed data ($p<0.0005$ for SUV_{max}; $p<0.0005$ for SUVmean; $p=0.003$ for lesion volume). The SUV results from *DDG-retro* were found to be significantly higher than *RPM-gated, Ungated matched, and Ungated full* on application of paired t-tests (Table 1). The differences between *DDG-retro* and *RPM-gated* were smaller than the differences between *DDG-retro* and *ungated matched* or *Ungated full*.

Radiologist scoring

From the 121 complete studies, the clinical evaluation revealed a significant difference in the image quality (rank) between the groups ($p<0.0005$). The same was true for the scores assigned for overall image quality ($p<0.0005$).

For most exams, the same score and rank was assigned to *RPM-gated* and *DDG-retro:* equal ranks on 102/121 occasions (85%), and equal scores of overall image quality on 114/121 occasions (94%). *DDG-retro* was preferred (better rank) over *RPM-gated* in 16 exams (13%),while in 3 exams (2%) *RPM-gated* was preferred over *DDG-retro*. This occasional preference for *DDG-retro* over *RPM-gated* was statistically significant (Wilcoxon Signed Ranks Test; $p=0.008$,$n=121$). A similar result was obtained for comparison of the scores of overall image quality ($p=0.008$).

Figure 3 shows the paired differences in scores of image quality. Out of the 121 complete datasets, the top ranked image was *ungated full* for 115 exams; this was a significant preference over *DDG-retro* (Wilcoxon Signed Ranks Test;$p<0.0005$,$n=144$). Although the *ungated matched* image was commonly ranked and scored equal with the respiratory gated images (equal rank to *DDG-retro* on 110 occasions; 76%), an overall preference for *DDG-*

retro over *ungated matched* was found to be statistically significant for ranks (Wilcoxon Signed Ranks Test; p=0.001, n=144) and image quality scores (p=0.002).

One or more lesions in the liver were identified in 23 of the 144 images. Considering this subset of data, *DDG-retro* was ranked superior to *ungated full* in 6/23 (26%) of cases. The overall preference for *ungated full* was not statistically significant (Wilcoxon Signed Ranks Test; p=0.067, n=23). There was a trend for *DDG-retro* to be preferred over *RPM-gated* in this subset of data (preference for *DDG-retro* in 7 exams, preference for *RPM-gated* in 2 exams; p=0.083, n=17). *DDG-retro* was preferred over *Ungated matched*, with a better rank in 13 cases, and with 8 ties (p=0.01, n=23). Paired differences in image quality for this dataset are presented in Figure 4. An example set of images is presented in Figure 5, with additional examples provided in Supplemental Figure 1.

Figure 6 provides an overview of the noise scores. Less noise was perceived in the *ungated full* images (with 6 minutes of data) as compared to the other three image sets (which each retained 3 minutes of data). These differences, observed for both the bone marrow and in the liver noise scores, were significant (Wilcoxon Signed Ranks Test; p<0.0005, n=143). The differences between the three reconstructions which retained 3 minutes of data were comparatively small.

Discussion

This study found a commercially developed data-driven respiratory gating algorithm to provide superior respiratory gating of PET data, as compared to gating using an external device in the setting of clinical ^{18}F-FDG PET-CT imaging. This superiority was demonstrated by a larger increase in SUV_{max} upon application of the respiratory gating, accompanied by improved clinical image quality. In 85% of cases the two methods of gating were considered to give images of equal quality when scored by a single, experienced radiologist, but with an occasional (13%) preference for DDG over RPM. Furthermore the data-driven gating had a lower failure rate. 100% of the *DDG-retro* images were considered to be clinically acceptable. For the 13/144 exams where the data-driven gating was unable to extract a suitable respiratory waveform, this did not prevent reconstruction of the PET images and did not introduce image artefacts. In the 23/144 (16%) exams where the external device failed, it produced errors in workflow or introduced low-count image artefacts due to missing respiratory triggers.

The study also indicates that quiescent period gating, with 50% of coincidences discarded, rarely provides an image considered superior in terms of image quality as compared to no gating with retention of all coincidences. The radiologist ranked respiratory gated images (*DDG-retro*) to be better than *ungated full* in just 9/144 exams (with no ties). Quiescent period gating (from a 6-minute acquisition) fared better when compared to no gating but from a shorter (3-minute) acquisition, with the gated images generally equivalent (tied rank 110/144, 76%) or preferred (superior rank 26/144, 18%). The preference for gated images over *ungated full* only occurred when disease was present in the abdominal organs, in which case there was a preference for gated images 26% of the time (superior rank, 6/23 exams). This occasional visual preference was accompanied by increased contrast (reduced

respiratory blurring) in the PET images upon application of the gating, as evidenced by an increase in SUV_{max} and SUV_{mean}, with a concurrent decrease in the threshold-defined lesion volume.

The primary measure under investigation in the study was SUV_{max}, chosen to remove subjectivity from the comparison. A radiologist assisted in the identification of lesions, but also provided clinical scoring that is expected to suffer from a bias towards a smoother image when there are no obvious abdominal lesions. The reduced noise leads to greater confidence of a lack of abnormality (such as small volume disease) in this region with a preference for this smoother image. Such an image may however be less optimal for diagnostic purposes, as demonstrated by the occasional visualisation of a liver lesion on the respiratory gated images which is absent from the non-gated, full count image (see Figure 5); in these specific cases it is of no surprise that the respiratory gated image received a superior score. The rate at which respiratory gated imaging is preferred is then dependent on the rate at which difficult-to-detect abdominal lesions are present in the patient population. Two important ramifications for patient care should be considered from these results: small abdominal lesions were generally clearer on gated images and hence respiratory gating has the potential to alter patient pathways (if gating is required for metastatic disease to be detected); SUV_{max} values were usually increased by respiratory gating and are likely more accurate, hence gating needs to be applied consistently in any disease monitoring investigations and in the definition of treatment thresholds based on SUV_{max}. In the current study we applied gating to all patients, rather than pre-selecting a subgroup of patients based on disease location or the amplitude of their respiratory motions.

The preference for DDG-retro over RPM-gated was likely a result of two factors. Firstly, the respiratory waveform derived from motion information contained in the PET data should be more representative of the motion of abdominal organs, as opposed to tracking the motion of the chest wall. Secondly, the data-driven technique determined the respiratory triggers after extraction of the whole respiratory waveform, as opposed to using a prospective triggering algorithm to insert respiratory triggers into the data-stream during acquisition.

A limitation of this study is its retrospective nature, together with the retrospective application of data-driven gating without any R-threshold to two pre-selected bed positions. Although the same DDG algorithm is used in MotionFree, we used the term “DDG-retro” to distinguish that we did not use the real-time R-threshold based application of DDG that is available within the MotionFree product (2019 release). The use of an R threshold would reduce the failure rate for DDG and is likely to assist in the selection of those specific patients (and bed positions) for which respiratory gating will be of benefit. There may have been bed positions more superior or inferior than the pre-selected ones that would have benefitted from respiratory gating. For the BPL image reconstruction, a fixed beta value of 400 was used for all four reconstructions and all bed positions; this value may be suboptimal for the 6-minute duration bed positions in the *Ungated full* reconstructions. We did not attempt to compare the commercially developed DDG algorithm with the other approaches to data-driven gating (15,16). For a detailed discussion of such methods, the reader is referred to previous publications (6,9,20).

Furthermore, in this study there was no attempt to improve the alignment of the free-breathing CT image with the quiescent-phase PET image. While images from the two modalities were often closely aligned, there were occasions where the CT exposure occurred at a different respiratory phase leading to mis-alignment of the images and the introduction of well recognised attenuation and scatter correction artefacts. Application of quiescent period gating in such a manner is known to cause changes in the magnitude of these artefacts with corresponding changes in lesion quantification (21). While this does not confound our comparison of DDG-retro and RPM-gated images (as both make use of the same CTAC and a similar respiratory phase for the PET data), it is a confounding factor for comparison of gated images and non-gated images, and hence the quantitative comparison we performed is subject to this caveat. A robust method to realign free-breathing CT datasets to those from respiratory gated PET could increase the benefits of respiratory gated PET imaging in the future.

Similarly, this study only considered quiescent-period gating as we primarily sought comparison of device-based and deviceless respiratory gating. Several manufacturers offer quiescent period gating, with different methods for identifying the part of the waveform to retain and with user-defined parameters to provide different retention fractions (e.g. 25–50%) (19,22). PET respiratory gating with retention of more than 50% of coincidences has been previously described (23,24) but the current methods are complex and rarely used in practice. Additional methods that retain a higher fraction of the coincidences are under development. This study suggests that retention of more than 50% of coincidences may be required before respiratory gated PET imaging can routinely and unequivocally outperform ungated PET imaging.

Conclusion

In the context of oncological ^{18}F-FDG PET/CT imaging, we conclude that a commercially developed, data-driven respiratory gating technique provided superior performance as compared to a commercially available, external device-based respiratory gating system. The data-driven method is likely to increase the utilisation of respiratory gating in clinical PET imaging due to superior performance and improved workflow.

Supplementary Material

Refer to Web version on PubMed Central for supplementary material.

Acknowledgments

DM is funded by a NIHR/HEE Clinical Lectureship.

References

1. Clifford MA, Banovac F, Levy E, Cleary K. Assessment of hepatic motion secondary to respiration for computer assisted interventions. Comput Aided Surg. 2002; 7:291–299. [PubMed: 12582982]
2. Bussels B, Goethals L, Feron M, et al. Respiration-induced movement of the upper abdominal organs: a pitfall for the three-dimensional conformal radiation treatment of pancreatic cancer. Radiother Oncol. 2003; 68:69–74. [PubMed: 12885454]

3. van der Vos CS, Koopman D, Rijnsdorp S, et al. Quantification, improvement, and harmonization of small lesion detection with state-of-the-art PET. Eur J Nucl Med Mol Imaging. 2017; 44:4–16. [PubMed: 28687866]
4. Pépin A, Daouk J, Bailly P, Hapdey S, Meyer M-E. Management of respiratory motion in PET/computed tomography: the state of the art. Nucl Med Commun. 2014; 35:113–122. [PubMed: 24352107]
5. Thielemans, K; Rathore, S; Engbrant, F; Razifar, P. Device-less gating for PET/CT using PCA. 2011 IEEE Nucl Sci Symp Conf Rec; 2011. 3904–3910.
6. Thielemans, K; Schleyer, P; Marsden, PK; Manjeshwar, RM; Wollenweber, SD; Ganin, A. Comparison of different methods for data-driven respiratory gating of PET data. 2013 IEEE Nucl Sci Symp Conf Rec; 2013. 1–4.
7. Bertolli O, Arridge S, Wollenweber SD, Stearns CW, Hutton BF, Thielemans K. Sign determination methods for the respiratory signal in data-driven PET gating. Phys Med Biol. 2017; 62:3204–3220. [PubMed: 28346222]
8. Walker MD, Bradley KM, McGowan DR. Evaluation of principal component analysis-based data-driven respiratory gating for positron emission tomography. Br J Radiol. 2018; 91
9. Walker MD, Morgan AJ, Bradley KM, McGowan DR. Evaluation of data-driven respiratory gating waveforms for clinical PET imaging. EJNMMI Res. 2019; 9:1. [PubMed: 30607651]
10. Morley NCD, McGowan DR, Gleeson FV, Bradley KM. Software respiratory gating of Positron Emission Tomography–Computed Tomography improves pulmonary nodule detection. Am J Respir Crit Care Med. 2017; 195:261–262. [PubMed: 27755923]
11. Rietzel E, Chen GTY, Choi NC, Willet CG. Four-dimensional image-based treatment planning: Target volume segmentation and dose calculation in the presence of respiratory motion. Int J Radiat Oncol Biol Phys. 2005; 61:1535–1550. [PubMed: 15817360]
12. Hoisak JDP, Sixel KE, Tirona R, Cheung PCF, Pignol J-P. Correlation of lung tumor motion with external surrogate indicators of respiration. Int J Radiat Oncol Biol Phys. 2004; 60:1298–1306. [PubMed: 15519803]
13. Li R, Mok E, Han B, Koong A, Xing L. Evaluation of the geometric accuracy of surrogate-based gated VMAT using intrafraction kilovoltage x-ray images. Med Phys. 2012; 39:2686–2693. [PubMed: 22559639]
14. Büther F, Jones J, Seifert R, Stegger L, Schleyer P, Schäfers M. Clinical evaluation of a data-driven respiratory gating algorithm for whole-body positron emission tomography with continuous bed motion. J Nucl Med. 2020 Feb 14.
15. Kesner AL, Chung JH, Lind KE, et al. Validation of software gating: a practical technology for respiratory motion correction in PET. Radiology. 2016; 281:239–248. [PubMed: 27027335]
16. Büther F, Vehren T, Schäfers KP, Schäfers M. Impact of data-driven respiratory gating in clinical PET. Radiology. 2016; 281:229–238. [PubMed: 27092660]
17. Bettinardi V, Presotto L, Rapisarda E, Picchio M, Gianolli L, Gilardi MC. Physical performance of the new hybrid PET/CT Discovery-690. Med Phys. 2011; 38:5394–5411. [PubMed: 21992359]
18. Teoh EJ, McGowan DR, Macpherson RE, Bradley KM, Gleeson FV. Phantom and clinical evaluation of the Bayesian penalized likelihood reconstruction algorithm Q.Clear on an LYSO PET/CT system. J Nucl Med. 2015; 56:1447–1452. [PubMed: 26159585]
19. Liu C, Alessio A, Pierce L, et al. Quiescent period respiratory gating for PET/CT. Med Phys. 2010; 37:5037–5043. [PubMed: 20964223]
20. Kesner AL, Kuntner C. A new fast and fully automated software based algorithm for extracting respiratory signal from raw PET data and its comparison to other methods. Med Phys. 2010; 37:5550–5559. [PubMed: 21089790]
21. Meier JG, Einstein SA, Diab RH, Erasmus LJ, Xu G, Mawlawi OR. Impact of free-breathing CT on quantitative measurements of static and quiescent period-gated PET Images. Phys Med Biol. 2019; 64
22. van Elmpt W, Hamill J, Jones J, De Ruysscher D, Lambin P, Ollers M. Optimal gating compared to 3D and 4D PET reconstruction for characterization of lung tumours. Eur J Nucl Med Mol Imaging. 2011; 38:843–855. [PubMed: 21222120]

23. Huang T-C, Chou K-T, Wang Y-C, Zhang G. Motion freeze for respiration motion correction in PET/CT: a preliminary investigation with lung cancer patient data. BioMed Res Int. 2014; 2014

24. Hong, I; Jones, J; Hamill, J; Michel, C; Casey, M. Elastic motion correction for continuous bed motion whole-body PET/CT. 2016 IEEE Nucl Sci Symp Conf Rec; 2016. 1–2.

Europe PMC Funders Author Manuscripts

Europe PMC Funders Author Manuscripts

Key Points

Question

How does data-driven respiratory gating, for ^{18}F-FDG PET/CT, perform in comparison to device-based respiratory gating?

Pertinent Findings

Blinded comparison of 144 ^{18}F-FDG PET/CT images found a significant preference for the data-driven respiratory gating technique over the device-based system, despite similar scores of image quality and similar quantification of lesions in the majority of patients.

Implications for Patient Care

The data-driven method is likely to increase the utilisation of respiratory gating in clinical PET, leading to fewer respiratory artefacts and potentially increasing diagnostic accuracy.

Europe PMC Funders Author Manuscripts

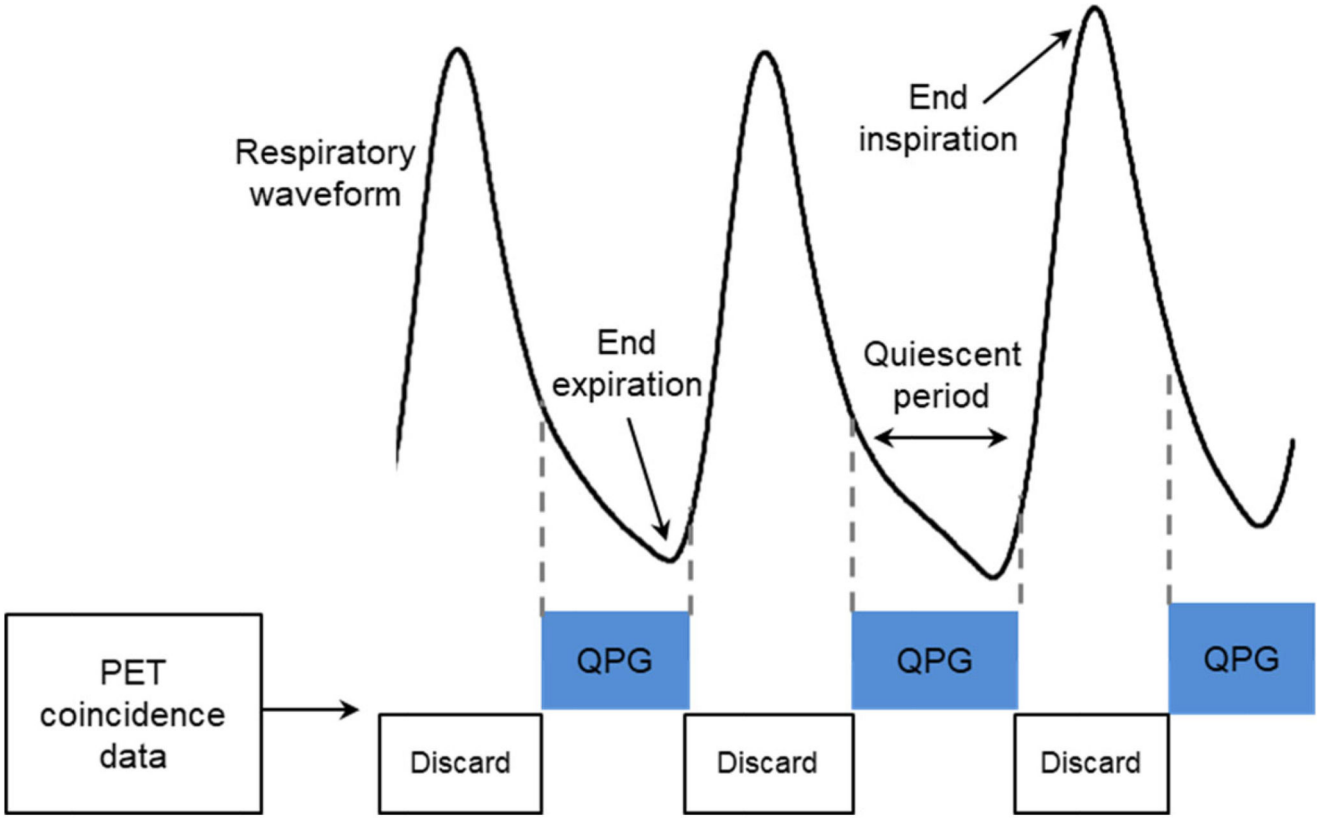

Figure 1.

A depiction of quiescent period gating, in which part of the respiratory cycle associated with relatively little motion is identified and retained in the gated image.

Europe PMC Funders Author Manuscripts

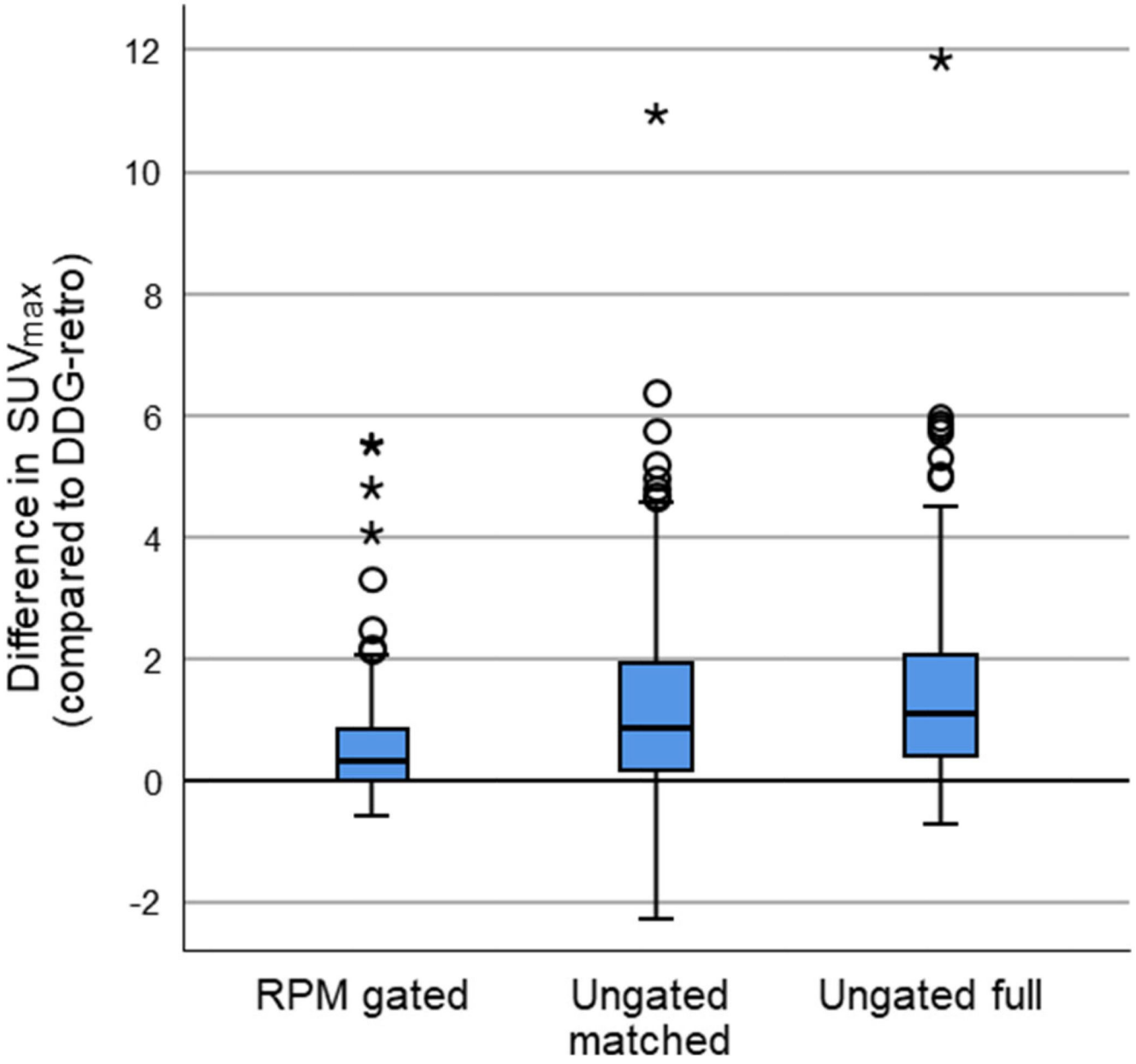

Figure 2.

Boxplots showing SUV_{max} for *DDG-retro*, minus that obtained from *RPM gated*, *Ungated matched*, or *Ungated full*. Positive values indicate higher SUV_{max} in the case of *DDG-retro*. The line on the box indicates the median.

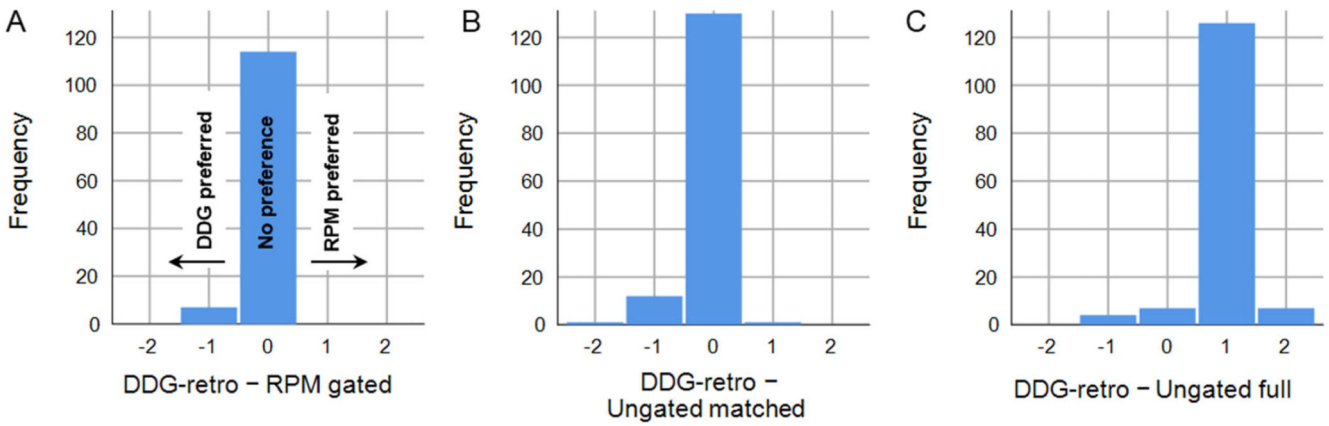

Figure 3.

Comparison of clinical scoring between *DDG-retro* and A) *RPM-gated*, B) *Ungated matched*, and C) *Ungated full*. A lower score indicated preference, and hence negative scores represent preference for *DDG-retro*.

Europe PMC Funders Author Manuscripts

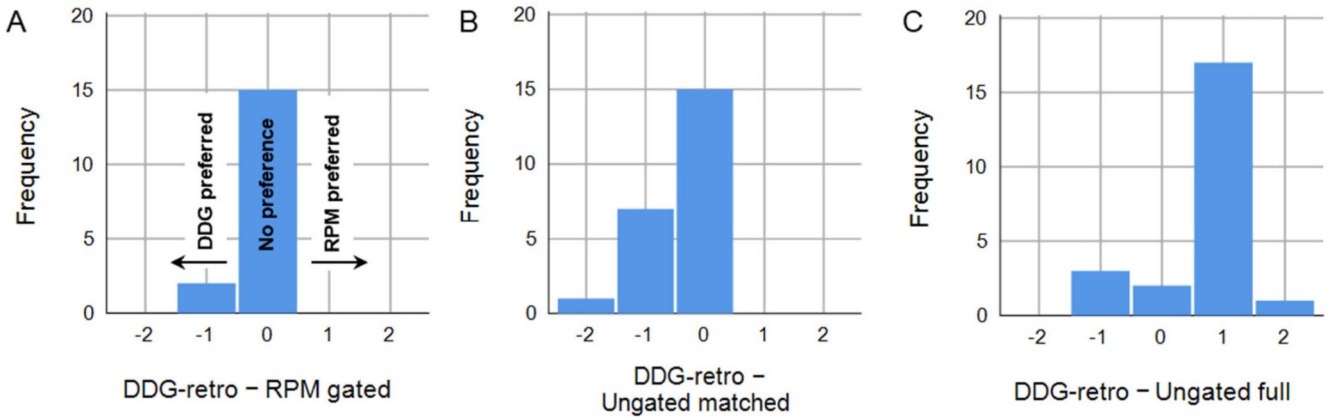

Figure 4.

Considering only those studies with visible lesions in the liver, a comparison of clinical scoring between *DDG-retro* and A) *RPM-gated*, B) *Ungated matched*, and C) *Ungated full*. A lower score indicated preference, and hence negative scores represent preference for *DDG-retro*.

Europe PMC Funders Author Manuscripts

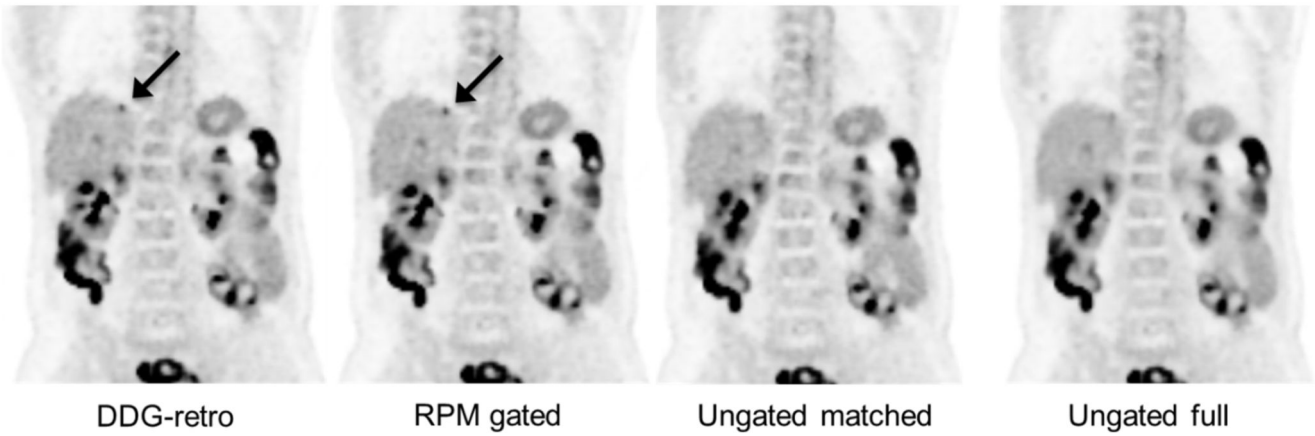

Figure 5.

A coronal slice showing an ^{18}F-FDG avid liver metastasis (indicated by arrow) which is easier to detect and has a higher SUV_{max} on the two gated reconstructions, as compared to ungated. In this example, the DDG-retro and RPM-gated images received an equal score for overall image quality, and both were considered superior to the ungated images. The lesion indicated by the arrow was not considered to be definitely visible on the Ungated matched image, and was borderline-visible on the Ungated full image. One can also see the reduction in noise in the Ungated full image, as compared to the other three images. The images are on an SUV grayscale of 0–6.

Europe PMC Funders Author Manuscripts

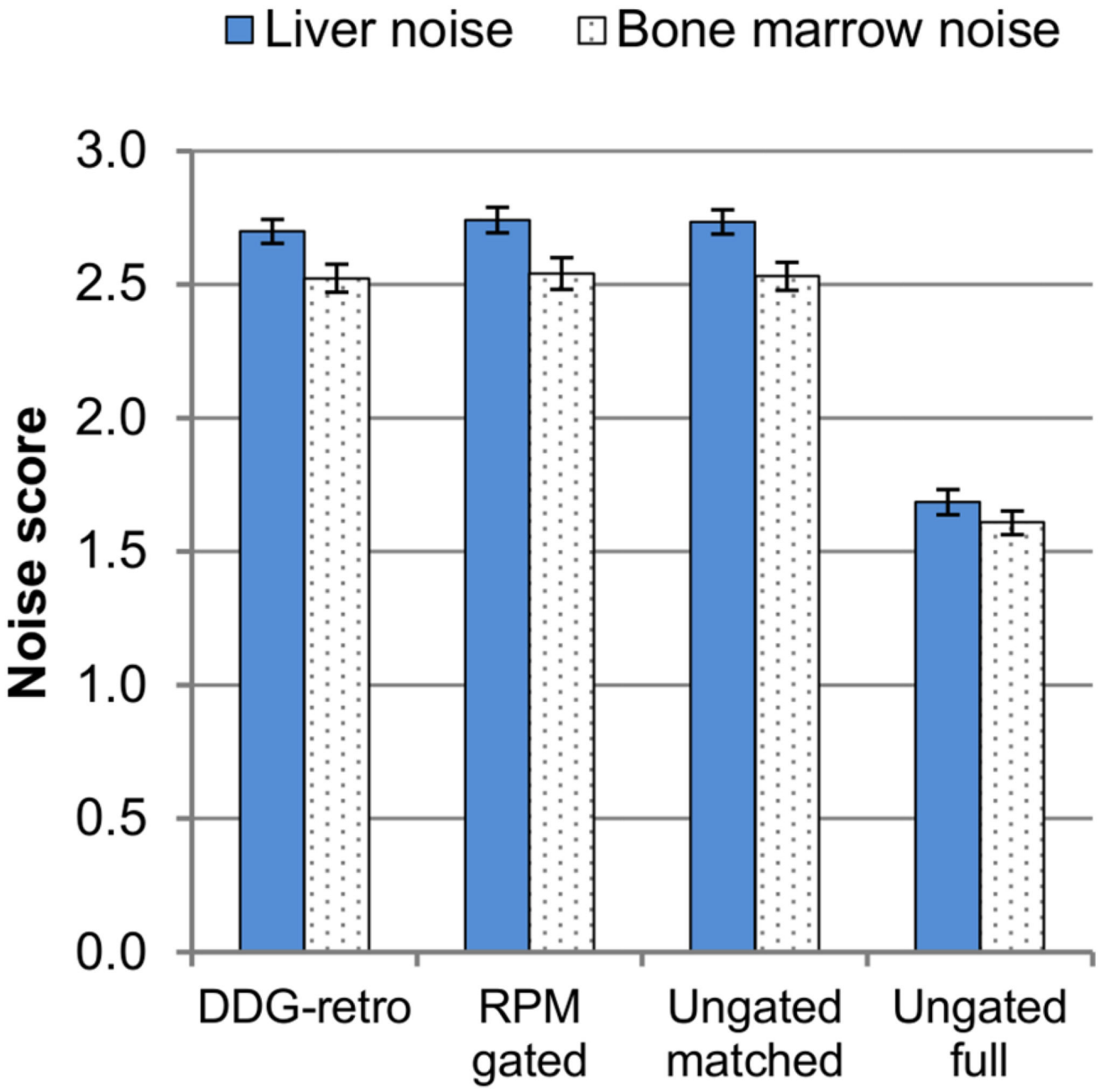

Figure 6.
Comparison of noise scoring across the four image reconstructions. Error bars represent standard errors on the mean.

Europe PMC Funders Author Manuscripts

Table 1

Differences in lesion quantification between *DDG-retro* and the three other methods of gating/reconstruction. Results are presented as mean differences (with standard error on the mean difference) along with the first and third quartile. The results from Post-hoc testing of the transformed data are also provided. The critical p value for statistical significance was 0.017 (lowered from 0.05 to allow for multiple comparisons).

Pairwise comparison *Parameter / DDG-retro with:*	**Number of lesions**	**Mean difference (*DDG-retro* – Other)**	**25th, 75th percentile on difference (DDG-*retro* – Other)**	**Significance (p; uncorrected for multiple comparisons)**
SUV max / RPM-gated	87	0.66 ± 0.1 g/mL	0.00, 0.87 g/mL	<0.0005
SUV max / ungated matched	107	1.3 ± 0.2 g/mL	0.06, 2.0 g/mL	<0.0005
SUV max / ungated full	107	1.6 ± 0.2 g/mL	0.38, 2.0 g/mL	<0.0005
SUV mean / RPM-gated	54	0.44 ± 0.1 g/mL	-0.01, 0.60 g/mL	0.003
SUV mean / ungated matched	64	0.97 ± 0.2 g/mL	0.01, 1.60 g/mL	<0.0005
SUV mean / ungated full	64	1.2 ± 0.2 g/mL	0.36, 1.59 g/mL	<0.0005
Lesion volume / RPM-gated	54	-0.30 ± 0.1 cm^3	-0.52, 0.03 cm^3	0.009
Lesion volume / ungated matched	64	-0.70 ± 0.2 cm^3	-0.98, -0.01 cm^3	0.005
Lesion volume / ungated full	64	-0.83 ± 0.2 cm^3	-1.05, -0.03 cm^3	0.001